Journal of New Technology and Materials (JNTM)
J. New Technol. Mater.
Vol. 12, N°02 (2022)35-42

OEB Univ. Publish. Co.

Evaluation of the solar potential of northern Algeria for use in a desiccant air-handling unit. Comparative study between several models

A. Bareche[a*] and N. Labed[b]

[a]*Laboratory of Materials, Structure of Electromechanical Systems, and their Reliability, University of Larbi Ben M'hidi, B.P. 358 Constantine Road, 04000, Oum El Bouaghi, Algeria*

[b]*University of Larbi Ben M'hidi, Oum El Bouaghi, Algeria*

*Corresponding author, email: amir.bareche@univ-oeb.dz

Received date: June 12, 2022 ; revised date: Oct. 2, 2022; accepted date: Oct. 19, 2022

Abstract

Within the framework of a project to realize a solar air-cooling plant by desiccation, a study for the estimation of the receivable solar potential at the level of a city in north Algeria is presented herein. Calculation codes have been performed for the cases of several horizontal irradiance models and then the predictions of these models were converted to global solar irradiation on inclined surfaces by the isotropic Liu and Jordan's method. The results were also tested in order to select statistically the closest ones to the experimental data collected in the city of La Rochelle in France. It was found that Capderou's model was the most accurate and therefore has been used in this study. The angle of inclination of the solar collectors has been fixed at 20° for a maximum capture during the whole summer season. The influence of the solar potential on the hot water storage capacity has been also discussed. The obtained results indicate that the quantity of captured energy will be sufficient for a correct regeneration of the desiccant in the air handing unit.

Keywords: Desiccant cooling; Solar radiation; Models; Potential; Air treatment

1. Preamble

The work describe in this paper is a part of an Algerian project program of realization of an air-cooling plant by desiccation with a solar regeneration (Figure 1). This technique which is relatively new, offers multiple energetic, economic and environmental advantages that makes it a serious alternative to conventional air treatment technologies. The viability of this technique depends essentially upon the quantity of solar energy captured and transformed.

Algeria and due to its geographical position, is a country with high direct solar irradiation (170kW/m^2/year) with, however, a great disparity between the different regions [1]. The duration of insulation varies from 2000 to 3900h/year, with a horizontal surface radiation of approximately 3 to 5 kWh/m^2 [1]. This study was carried out in order to quantify especially the usable solar potential in this case. A several calculation models results were used for a comparison with measured radiation data.

2. Introduction

In literature, many solar radiation assessment models have been developed and proposed for horizontal and sloping surfaces [2,3]. Generally speaking, models for horizontal surfaces are highly dependent on the availability of data measured by meteorological stations or satellite imagery [4]. Empirical, broadband or spectral models are available. However, radiation data on inclined surfaces studies are rather few [5], especially in developed countries, such as Algeria, due to their high costs and limited measurement techniques.

In this research work, and in order to evaluate the performances of several calculation models with the aim of assessing the exploitable solar potential on a tilted surface in the city of Oum El Bouaghi (Algeria), data measured at the LaSIE of La Rochelle University (France) [6] have been used. Furthermore, it will also be necessary to determine the angle of inclination that will ensure the ideal capture during the summer period. The purpose is, as explained above, to acquire viable data on the quantity of solar energy captured to be able to be used in the characterization of the air-handling unit by desiccation.

3. Bibliographic review

The early solar potential estimation studies are relatively old and very abundant. These are usually based on the value of solar radiation outside the atmosphere. At the ground level, the global solar radiation on the horizontal plane is defined as a combination of two components: direct and diffuse. Furthermore, for the case of an inclined plane, it is necessary to take into account the radiation reflected by the ground. The knowledge of the values of the global solar radiation components on the horizontal surfaces allows to deduce those of the inclined surfaces. For both, the direct and reflected components, this transition can be handled by relatively simple geometrical relationships. This is not true for the diffuse component, since the diffuse radiation does not have a defined or singular incidence angle.

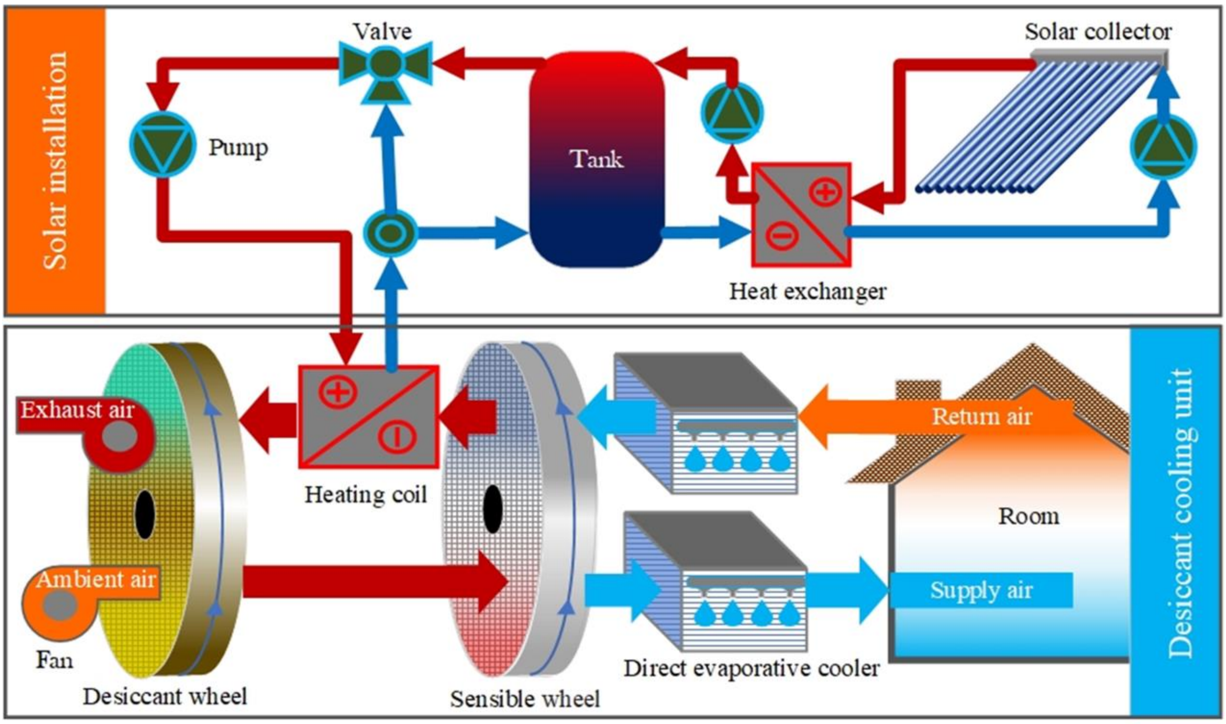

Figure 1. Principle chart of the air-cooling installation by desiccation with solar regeneration of LaSIE in La Rochelle

The dependence of empirical models on correlations between solar radiation and meteorological parameters limited their use [7–9]. Nevertheless, broadband models are based on both atmospheric and astronomical parameters. They have been used since the seventies of the XX century based upon the assumption of a clear sky, which is, normally the case as the air-cooling installation operates only during the summer season. The broadband models are, in principle, perfectly suited for this study.

Alam et al [10] analyzed three broadband models for four Indian measurement stations. They concluded that the REST model is better. Badescu et al [2] tested and presented a total of 54 models applied in Romanian sites. In their conclusions, they state that the ESRA, Ineichen, METSTAT, and REST2 models, give the best results for global solar radiation calculation.

Gueymard et al [11] evaluated an overall of 18 broadband models by comparing with experimental data. According to their study, the ranking in order of relevance of these models can be done as follows: REST2, Ineichen, Hoyt, Bird, and Iqbal-C. It should be noted that these models require a relatively large number of atmospheric inputs. For the Algerian particular case, Benkaciali et al [4] studied 18 broadband models to estimate direct solar radiation over two Algerian sites; They find that the Dogniaux model gives better results for Algiers city (in north of Algeria) while the ESRA for the city of Ghardaia (in south of Algeria).

To pass from global solar radiation on a horizontal plane to a sloping plane, the existing methods are of two types: Isotropic and anisotropic. The isotropic method of Liu and Jordan [12] has been validated by several studies [13,14]. Similarly, in a comparative study by Pandey et al [15], the anisotropic method of Klosher [16] provided best estimation of solar potential on inclined surfaces in India.

4. Models used

As part of this study, and for simulation reason of the received solar radiation following ten different horizontal irradiance clear sky models, ten computer programs under MATLAB developed to select the closest experimental data collected at the LaSIE (Figure 3).

The Braodband models have been chose and used as they fit better with the objective of this study. The MAC [17], Yang [18], CPCR2 [19] and REST2 [20] models whose basic functional form is similar to the Bird [21], and REST [22] models mentioned in section4.2, 4.3. The main difference between these models lies in the number of transmittance functions and the used atmospheric inputs. In CPCR2 and REST2 which are two-band models in which the solar spectrum is divided into a UV/visible band (0.29-0.7µm) and an infrared band (0.7-2.7µm). The

Ashrae model [23] is a simple one based solely on experimentally determined constants. The calculation with these models gave interesting results, but the models below are more relevant in terms of results. Therefore, we are going to devote more explanation to them.

4.1. Capderou model

Capderou is the basic model of the Algerian Solar Radiation Atlas. According to this model [24,25], the direct and diffuse solar radiation incident on horizontal surfaces are calculated using the atmospheric Linke's turbidity factor (T_L), the values of this factor can be determined only from geographical and astronomical parameters (altitude *z*, latitude φ, solar elevation *h*, and day number j). Capderou gives the horizontal global solar radiation as follows:

$$G_h = B_h + D_h \tag{1}$$

$$B_h = I_0 Ct \exp\left[-T_L\left(0.9 + \left(9.4/0.89^z\right)\sin h\right)^{-1}\right]\sin h \tag{2}$$

$$D_h = I_0 Ct \exp\left[1 + ln\left(\sin h\right)\right] - \sqrt{1.21 + a^2} \tag{3}$$

$$a = ln\left(T_L - T_0\right) - 2.8 + 1.02\left(1 - \sin h\right)^2 \tag{4}$$

Where, G_h, B_h, D_h are the global, direct and diffuse radiation on a horizontal surface, I_0 the solar constant (I_0=1365 W/m^2), *Ct* the correction of the Earth–Sun distance and T_0, is the gaseous absorption factor.

4.2. Bird model

In this model, the direct solar radiation in this model [21] is the simple product of five broadband transmissions: Rayleigh scattering (T_R), mixed gas absorption (T_g), ozone absorption (T_o), water vapor absorption (T_w), and aerosol extinction (T_a). Furthermore, the diffusing component is the sum of the solar irradiance from atmospheric scattering (D_{as}) and the solar irradiance from multiple reflections between the ground and sky (D_g). The direct and diffuse radiation on a horizontal surface are calculated in the following manner:

$$B_h = 0.9662 Ct I_0 T_o T_R T_w T_g T_a sin\left(h\right) \tag{5}$$

$$D_h = D_{as} + D_g \tag{6}$$

$$D_{as} = 0.79 I_0 T_o T_w T_g T_{aa} sin\left(h\right) \left[0.5\left(1 - T_R\right) + B_a\left(1 - T_{as}\right)\right] / \left(1 + M_a + M_a^{1.02}\right) \tag{7}$$

$$T_{as} = T_a / T_{aa} \tag{8}$$

$$D_g = \left(B_h + D_{as}\right) / \left(1 - \rho_g \rho_a\right) \tag{9}$$

$$\rho_a = 0.0685 + \left(1 - B_a\right)\left(1 - T_a\right) \tag{10}$$

Where T_{aa} is the transmittance of direct radiation due to aerosol absorption, T_{as} is the incident energy fraction transmitted after the scattering aerosols effects, M_a is the air mass, ρ_g is the Ground albedo, ρ_a is the Albedo of the cloudless sky and B_a is the Ratio of the forward-scattered irradiance to the total scattered irradiance due to aerosols.

4.3. REST model

This model named "Reference Evaluation of Solar Transmittance" [22]. Like Bird, REST is also based on the same broadband transmissions along with the absorption of nitrogen dioxide (T_n) in the computation of direct solar irradiance. As the model deals only with direct radiation, the Bird method has been included (see Section 4.2) to achieve the whole calculation of diffuse radiation, which was not include in the original paper.

$$B_h = I_0 Ct T_R T_g T_o T_n T_w T_a \sin h \tag{11}$$

4.4. Ineichen model

This broadband model has been created to reduce the computational time of the RTM "Radiative Transfer Model " [26], especially for the assessment of solar radiation over a large area. In addition to the geo-astronomical parameters, Ineichen, which also, depends on the atmospheric aerosol optical depth and water vapor column for modelling the global solar radiation components, which are presented below:

$$B_h = I_0^{'} Ct \exp\left(\tau_b / \sin^b h\right)\sin h \tag{12}$$

$$D_h = I_0^{'} Ct \exp\left(\tau_d / \sin^d h\right)\sin h \tag{13}$$

Where I'_0 modified extra-terrestrial irradiance, τ_b and τ_d are the direct and diffuse total optical depths respectively, *b* and *d* the corresponding fitting parameters obtained upon RTM calculations.

4.5. R.sun model

This model [27] arises from the European Solar Radiation Atlas, based on geographical information systems (GIS). The R.sun model has also been used in the topographic mapping of solar radiation over Europe and Africa [11]. The estimation of the direct and diffuse components on a horizontal surface in this model is based upon the Linke turbidity factor. The turbidity factor's values for various landscapes in the world can be found in soda (http://www.soda-is.com).

$$B_h = I_0 Ct \sinh \exp\left(-0.8662 T_L M_a \delta_R\right) \tag{14}$$

$$D_h = I_0 Ct T_n\left(T_L\right) F_d\left(h\right) \tag{15}$$

Where δ_R the Rayleigh optical thickness, T_d the diffuse transmission function depends only on the Linke turbidity factor, F_d the diffuse solar altitude function depends only on the solar elevation.

4.6. Inclined solar radiation methods

The global solar radiation incident on a surface facing south and inclined at an angle (β) with respect to the horizontal plane is expressed by:

$$G_i = B_h R_b + D_h R_d + G_h R_r \tag{16}$$

The expression $G_h R_r$ gives the radiation reflected from the ground R_b, R_d and R_r are the conversion factors, they represent the ratios between the direct, diffuse and reflected hourly radiation on a tilted surface and that on a horizontal surface [26]:

$$R_b = \frac{\sin\delta\sin(\varphi-\beta)+\cos(\varphi-\beta)\cos\delta\sin W}{\sin\delta\sin(\varphi)+\cos(\varphi)\cos\delta\sin W} \tag{17}$$

$$R_r = \rho_g\left(1-\cos\beta\right)/2 \tag{18}$$

The chosen methods to determine the conversion factor R_d are the isotropic method of Liu and Jordan [13] (Eq. 19), and the anisotropic method of klocher (Eq. 20)

$$R_d = \left(1+\cos\beta\right)/2 \tag{19}$$

$$R_d = \left[\left(1+\cos\beta\right)/2\right]\left[1+f\sin^3\left(\beta/2\right)\right]\left[1+f\cos^2\theta\sin^3\left(90-h\right)\right] \tag{20}$$

$$f = 1-\left(D_h/G_h\right)^2 \tag{21}$$

$$\cos\theta = \sin\delta\sin(\varphi-\beta)+\cos(\varphi-\beta)\cos\delta\sin W \tag{22}$$

Where W is the hour angle, δ is the solar declination, f is the modulation function and θ is the incidence angle.

5. Methodology

For each of the 10 retained models, and based on geographical data (Table 1), the needed atmospheric parameters are calculated. Using the horizontal solar radiation models, the global, direct and diffuse components on a horizontal surface are also determined. On days of calculation, the components on a 45° inclined plane are deduced using an isotropic method of Liu and Jordan. The anisotropic method of Klosher showed poor results. The reflected component of the inclined plane is a function of the horizontal global radiation, while the inclined direct and diffuse are inferred directly from horizontal values Figure 2.

The experimental results [6] are used for the evaluation of the studied models described in this paper. The accuracy of each model is checked with the assistance of the most used statistical methods, that is the relative root mean squared error (rRMSE), mean bias error (MBE), the root mean squared error (RMSE), and the coefficient of determination (R^2), which express respectively the long-term and short-term model performances, the linear relationship between the measured and calculated values [24]. The more accurate model will be used to calculate the solar potential available in the city of Oum El Bouaghi (Algeria) (Table 1). The tilt angle of the solar collector is also chosen to ensure the maximum capture of solar radiation during the entire period of the air-cooling system operation (summer). The calculation is performed for the selected days from 10 am to 7 pm with a time step of 1 minute. We have:

$$RMSE = \frac{\left[\sum_{k=1}^{N}\left(G_{i,k}-G_{m,k}\right)^2\right]^{0.5}}{N} \tag{23}$$

$$rRMSE = \frac{RMSE}{G_{m,a}}100\% \tag{24}$$

$$MBE = \frac{1}{N}\sum_{k=1}^{N}\left(G_{i,k}-G_{m,k}\right) \tag{25}$$

$$R^2 = \frac{\left[\sum_{k=1}^{N}\left(G_{i,k}-G_{i,a}\right)\left(G_{m,k}-G_{m,a}\right)\right]^2}{\sum_{k=1}^{N}\left(G_{i,k}-G_{i,a}\right)^2\sum_{k=1}^{N}\left(G_{m,k}-G_{m,a}\right)^2} \tag{26}$$

Where, $G_{i,k}$, $G_{m,k}$, $G_{i,a}$ and $G_{m,a}$ are the estimated and measured values, the mean of estimated and measured values, respectively.

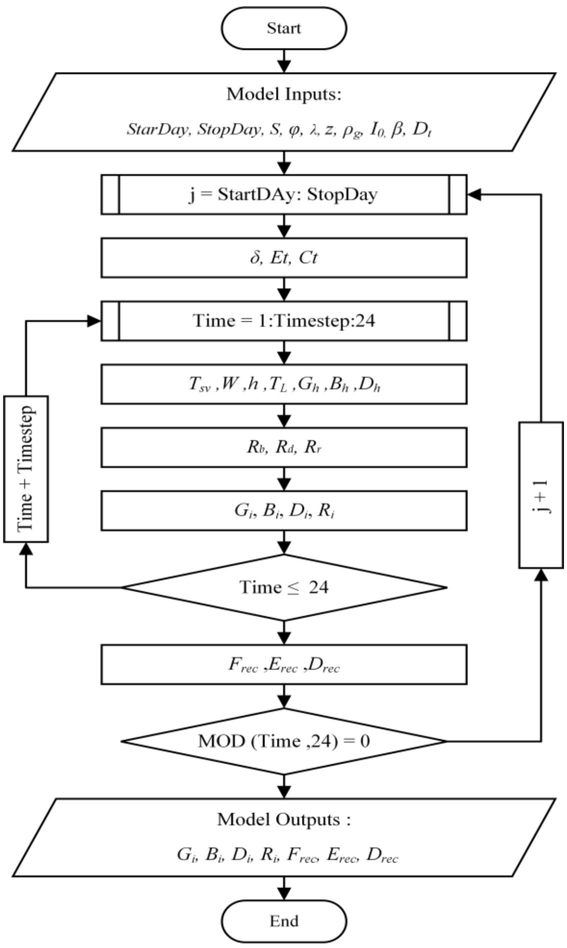

Figure 2. Summarized and simplified organizational flow-chart for Capderou model

Where S is the collector area, Dt the difference between local and standard time, Et the equation of time, T_{sv} is the true solar time, F_{rec} the flux solar received, E_{rec} the average energy received, and D_{rec} is the daily energy received.

Table 1: Geographic coordinates of the studied sites

Coordinates	La Rochelle (France)	Oum El Bouaghi (Algérie)
Latitude	46°16' N	35°87' N
Longitude	1°15' W	7°12' E
Altitude	10 m	900 m

6. Experimental data

The experimental data were acquired from tests performed on the desiccation air handing unit at the University of La Rochelle in France. A full-size installation of with 40 m² of high-performance vacuum solar panels, oriented to the south with an inclination of 45° [6]. Dates of July 17 and September 8 because of their favorable climatic conditions have been chosen (Figure 4).

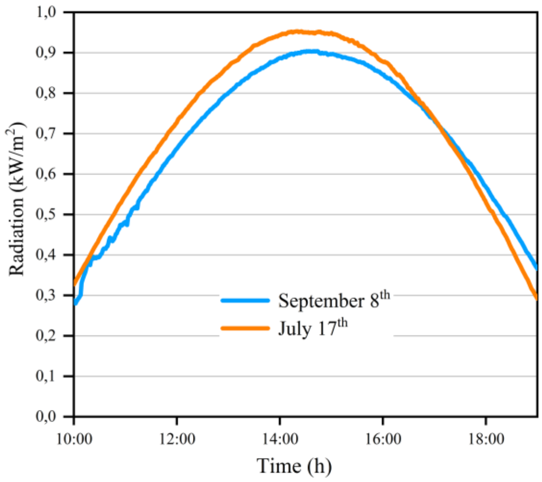

Figure 3. Global solar flux curves in La Rochelle

7. Results

7.1. Discussion of results of all simulation models

Table 2 : presents the statistical results for all used models. The calculation is performed in two steps. The first step consists of the determination of the global horizontal solar flux that will be transformed, in the second step, into radiation on a surface inclined at 45° using the isotropic model. The differences are calculated by comparing the results with the experimental data. The Ineichen model gives the minimum error for July 17th yet the Yang model gives the maximum. For September 8th, most models have given satisfactory results. It has been noticed, for example, that MAE is practically zero for the CPCR2 model, six models have the relative root mean squared error rRMSE lower than 2.5% and the coefficient of determination R^2 close to 1, the Capderou model is among the four models that offers the best predictions for both days.

In figure 4 a comparison between the calculation following the chosen models and the experimental data is displayed. The general shape of the curves is respected, but the results of September the 8th are the best as it can be noticed from (Figure 4). The deviations between models and experimental data are presented in figure 5. As shown in figure 5, most models offer absolute deviations below 50W/m² with a consistency throughout the day on September 8th. For July the 17th, the error is significantly larger since the majority of results are below 100 W/m². It is thought that this is due most likely to the climatic conditions in which the measurement was made (unclear sky).

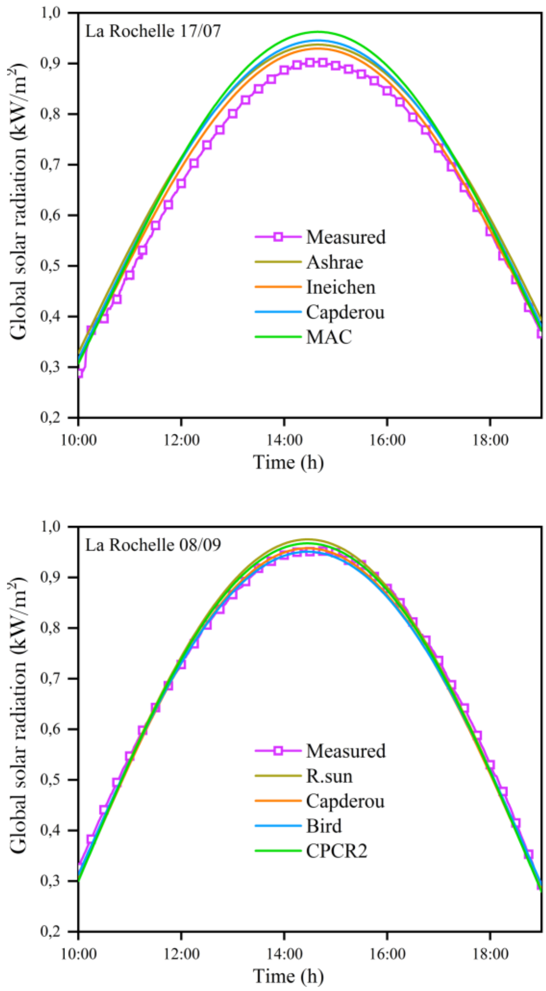

Figure 4. Comparisons between measured and estimated daily global solar radiation

7.2. Selection of working models

Statistical deviations for each model are calculated and then compared to the experimental data (Table 3). Broadly speaking, it was found that the results of the isotropic method are better than the anisotropic ones. The mean bias error MBE for all models ranges from 5.622 to 50.19 W/m²; while the relative root mean squared error rRMSE varieties from 4.211 to 9.401%. A full comparison of the obtained results, including all statistical indicators, clearly demonstrates that the Capderou model as it gives the best results. In other words, its performance test values are satisfactory. In the long term, the mean bias error is MBE=13.44 W/m² and RMSE=28.21 W/m². In the short term, the relative root mean squared error rRMSE does not exceed 4%, and R^2 is close to 0.98 (the ideal value of this indicator is 1). Therefore, the Capderou model will be adopted to estimate the solar radiation over the city of Oum El Bouaghi.

Table 2: Statistical results for the selected days using the isotropic method

Models	July 17				September 8			
	MBE (W/m2)	RMSE (W/m2)	rRMSE (%)	R2 (-)	MBE (W/m2)	RMSE (W/m2)	rRMSE (%)	R2 (-)
Ashrae	36.87	38.31	5.524	0.9537	31.97	35.38	4.883	0.9716
R.sun	41.77	43.76	6.309	0.9439	3.998	15.77	2.177	0.9943
Ineichen	20.47	23.70	3.417	0.9832	-47.87	48.79	6.734	0.9405
Capderou	34.92	37.33	5.382	0.9593	-8.031	14.06	1.941	0.9953
MAC	40.69	45.46	6.554	0.9452	-7.715	17.48	2.413	0.9929
Yang	101.5	102.	14.72	0.6579	24.31	25.63	3.537	0.9831
Bird	49.82	50.86	7.334	0.9186	-7.920	11.59	1.599	0.9966
REST	58.50	60.49	8.721	0.8968	-6.273	15.99	2.208	0.9941
CPCR2	76.66	77.73	11.21	0.8225	-1.251	14.16	1.954	0.9954
REST2	42.39	44.26	6.381	0.9424	-40.01	41.05	5.666	0.9557

Table 3: Statistical results for both days using the both irradiance methods on the inclined surface

Models	Isotropic Method (Liu and Jordan)				Anisotropic Method (Klucher)			
	MBE (W/m2)	RMSE (W/m2)	rRMSE (%)	R2 (-)	MBE (W/m2)	RMSE (W/m2)	rRMSE (%)	R2 (-)
Ashrae	34.42	36.88	5.201	0.9643	57.64	60.57	8.542	0.9048
R.sun	22.88	32.89	4.638	0.9723	53.61	63.20	8.913	0.9013
Ineichen	-13.70	38.36	5.409	0.9603	21.03	51.7	7.299	0.9319
Capderou	13.44	28.21	3.978	0.9792	42.27	54.92	7.745	0.9247
MAC	16.49	34.44	4.857	0.9708	38.35	53.27	7.513	0.9013
Yang	62.95	74.44	10.49	0.8427	128.03	141.09	13.04	0.4902
Bird	20.95	36.89	5.202	0.9622	59.585	73.12	10.31	0.8576
REST	26.11	44.240	6.239	0.9509	61.58	77.47	10.92	0.8563
CPCR2	37.70	55.87	7.879	0.9207	89.90	107.75	15.19	0.7322
REST2	1.189	42.69	6.020	0.9504	40.62	70.36	9.922	0.8760

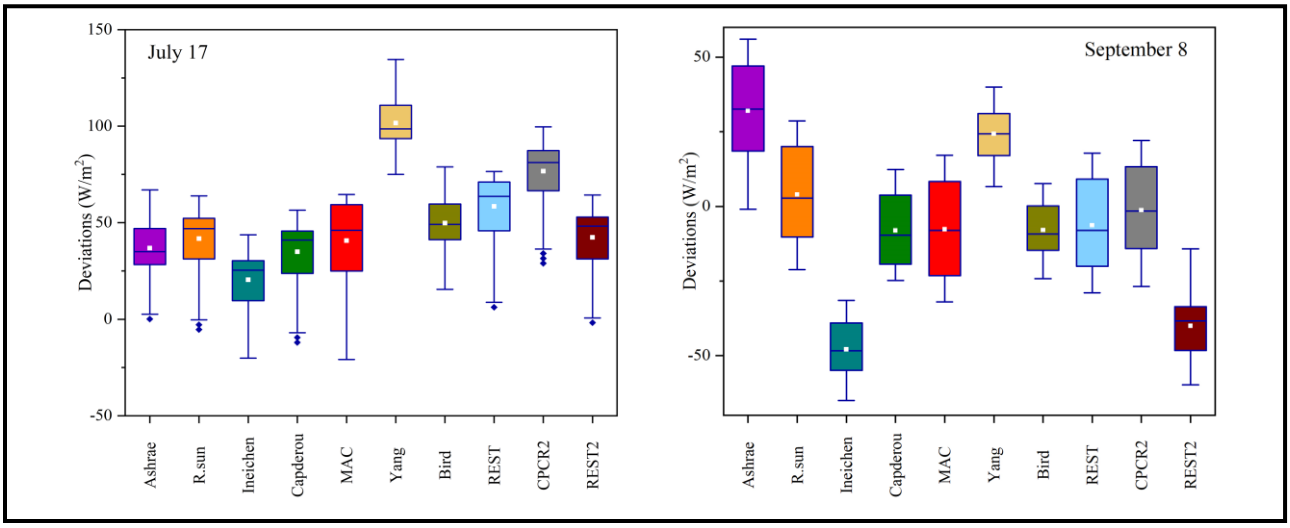

Figure 5. Scatter plot of the error for all the models used

7.3. Optimum slope angle

The slope of the angle of the solar collectors has a significant influence on the quantity of the received energy. The calculations were performed of the total energy captured and the maximum daily solar potential in Oum El Bouaghi using the selected model over the entire summer period. The tilt angles of 10° to 20° provide maximum solar radiation capture during the summer season (Figure 6). The 15° angle offers a captured energy of up to 758 kWh/m² but it is insufficient during the last days of the summer. The 20° angle value chosen, seems more stable and ensures a maximum flux of more than 1010 W/m² during the whole summer season.

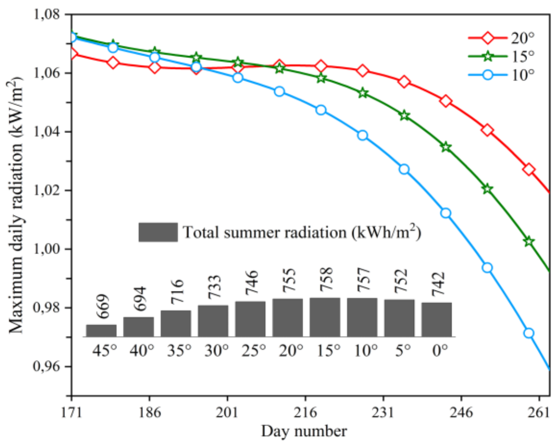

Figure 6. Influence of the slope angle on the quantity of solar energy received in the city of Oum El Bouaghi

8. Influence of the solar energy captured on the stored and used heat

In order to complete this study, it was decided to investigate the influence of the quantity of heat collected at the solar collectors on the hot water storage capacity and thus on the efficiency of the desiccant regeneration. For this purpose, TRNSYS software [28] has been used to simulate the operation of the DHU(Desiccant handing unit) of the University of La Rochelle (Figure 1). The main objective is to calculate the efficiency of the proposed solar system as well as the behavior of the heat stock available for the regeneration.

The simulation model (see Appendix A) consists of two circuits: Collectors ⇔ Heat Exchanger and Heat Exchanger ⇔ Storage Tank. Both are powered by two pumps and controlled by a regulator. Table 4 gives the input parameters of the main components.

The results of the full day simulation for the La Rochelle and Oum El Bouaghi sites are depicted in Figure 7.

Table 4: Parameters used in TRNSYS simulation

Component	TRNSYS Type	Component parameters
Evacuated Tube Collector	Type71	Environment temperature: 20°C, Number in series: 15, Total area: 42m², Slope: 45°, efficiency factor: 0.75
Heat Exchanger	Type91	Constant effectiveness: 0.8
Storage Tank	Type38	Initial temperature: 20°C, Volume: 2.75m³, height: 2.3m, Tank loss coefficient: 3 kJ/h. m².K, flow rate to load: 0 kg/s.
Pump	Type3b	Flow rate: 0.2 kg/s.

It is clear from Figure 7 that the same curves are obtained in the morning for both sites. At the beginning of the afternoon (Figure 7a), the temperature of the water at the tank inlet exceeds 80°C in both cases but it is even higher for the site of Oum El Bouaghi. At the end of the afternoon, the temperature drops due mainly to the lack of radiation and consequently the tank is no longer fed to preserve its stock. Storing the heat without exploiting it (for 11 hours) allowed to raise the average temperature of the thermal tank from 20°C to 70°C for La Rochelle and up to 75°C for Oum El Bouaghi and thus offering good conditions for the regeneration of desiccant of the DHU. The effective return of the installation is presented in Figure 7b. About 56% of the received solar energy is stored in the hot water tank. As far as the energy is concerned, the site of Oum El Bouaghi receives daily from 315 kWh; which is 10% more than La Rochelle.

Bourdoukan's experimental works [29], it was concluded that the DHU of La Rochelle requires a solar regeneration power of at least 20 kW to be effectively efficient. Calculation performed in this particular study indicates that, even counting for the possible heat losses of the tank (loss of about 20% of energy gained), the stored power (190 kWh/day for a collector inclination of 20 °) can effectively supply the DHU for 7 hours during the entire summer season (against 6 hours in La Rochelle). Other Algerian cities belonging to different geographical situations in the country have also been tested: Table 5.

Table 5: Results of some sites in north Algeria for 40 m² of solar collectors with a slope angle of 20°

Site	Constantine	Bouzareah	Oran	Biskra
Latitude	36°83' N	36°8' N	35°7' N	34°8' N
Longitude	6°62' E	3' E	0°65' W	5°73' E
Altitude (m)	694	345	22	87
Total flux received in summer (kWh/m²)	745	723	701	704

Average energy received (kWh/ m²/day)	8.01	7.77	7.54	7.57
Average energy stored (kWh/day)	188	183	177	178
Average regeneration time (hours/day)	7.5	7.3	7	7.1

Note: In the above results, the summer season has been adopted from June 21th to September 21th

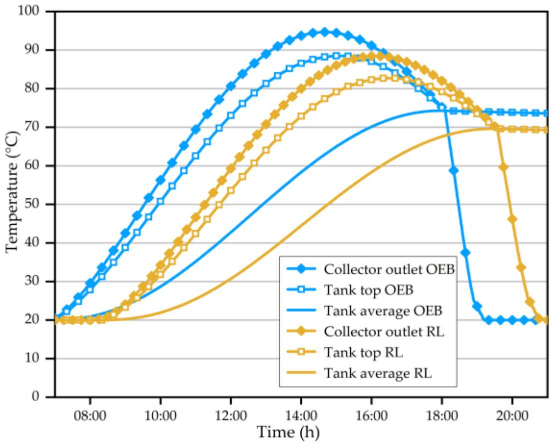

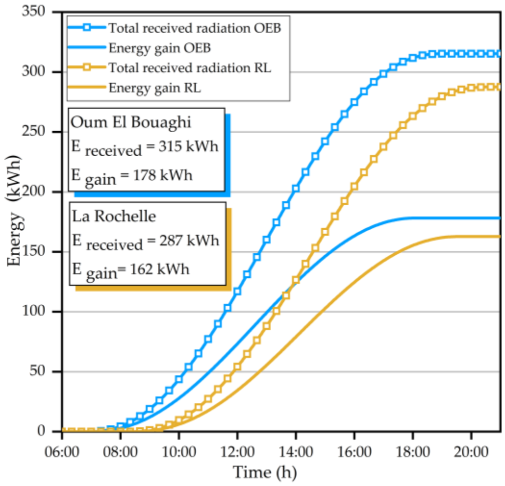

(b)

Figure 7. Temperature (a) and energy (b) predictions of solar installation components for the day of September 8th

9. Conclusion

In this particular study, the objective of quantifying the solar potential available to power in a desiccant air-cooling plant a total of ten computational models have been used and tested. From the results of this study, some interesting conclusions may be drawn. It was found that Capderou model gives better results as compared to the experimental data results and statistical methods outcomes. It was then associated with Liu & Jordan's model to calculate the solar radiation received at the level of the city of Oum El Bouaghi by a collector oriented towards the south and inclined with 20°. Furthermore, calculations performed in this study indicates that the quantity of energy received during the entire summer season (June 21th to September 21th) is 755 kWh/m² or an average of 8.1 kWh/m²/day. A simple calculation of the order of value shows that this quantity will be sufficient for the regeneration of the desiccant material of a plant in the city of Oum El Bouaghi. Also, these results can help to modulate the real operation of an air-cooling.

References

[1] Y. Zahraoui, M.R. Basir Khan, I. Alhamrouni, S. Mekhilef, M. Ahmed, Energies 14 (2021).
[2] V. Badescu, C.A. Gueymard, S. Cheval, C. Oprea, M. Baciu, Renew. Sustain. Energy Rev. 16 (2012) 1636–1656.
[3] C. Demain, M. Journée, C. Bertrand, Renew. Energy 50 (2013) 710–721.
[4] S. Benkaciali, M. Haddadi, A. Khellaf, Renew. Energy 125 (2018) 694–711.
[5] A.A. El-Sebaii, F.S. Al-Hazmi, A.A. Al-Ghamdi, S.J. Yaghmour, Appl. Energy 87 (2010) 568–576.
[6] N. Labed, P. Joubert, M. Burlot, Rev. Générale Du Froid (2018) 32–39.
[7] A. Louche, G. Notton, P. Poggi, G. Simonnot, Sol. Energy 46 (1991) 261–266.
[8] H. Duzen, H. Aydin, Energy Convers. Manag. 58 (2012) 35–46.
[9] R.G. Makade, S. Chakrabarti, B. Jamil, Urban Clim. 29 (2019).
[10] S. Alam, Renew. Energy 31 (2006) 1253–1263.
[11] C.A. Gueymard, Sol. Energy 86 (2012) 2145–2169.
[12] A. De Miguel, J. Bilbao, M. Diez, Energy Convers. Manag. 36 (1995) 945–951.
[13] S. Nijmeh, R. Mamlook, Renew. Energy 20 (2000) 75–81.
[14] K. Bakirci, Renew. Sustain. Energy Rev. 16 (2012) 6149–6159.
[15] C.K. Pandey, A.K. Katiyar, Appl. Energy 88 (2011) 1455–1459.
[16] T.M. Klucher, Sol. Energy 23 (1979) 111–114.
[17] J.A. Davies, D.C. McKay, Sol. Energy 29 (1982) 55–64.
[18] K. Yang, G.W. Huang, N. Tamai, Sol. Energy 70 (2001) 13–22.
[19] C. Gueymard, Sol. Energy 43 (1989) 253–265.
[20] C.A. Gueymard, Sol. Energy 82 (2008) 272–285.
[21] R.E. Bird, R.L. Hulstrom, Sol. Energy Res. Inst. 7 (1981) 1–16.
[22] C.A. Gueymard, Sol. Energy 74 (2003) 355–379.
[23] N. Nijegorodov, Renew. Energy 9(1996) 1270–1273.
[24] Y. El Mghouchi,A. El Bouardi, Z. Choulli, T. Ajzoul, Renew. Sustain. Energy Rev. 56 (2016) 87–99.
[25] I. Fellak, M. El Ganaoui, A. Mimet, A. Maalouf, Energy Procedia 139 (2017) 180–185.
[26] P. Ineichen, Sol. Energy 82 (2008) 758–762.
[27] J. Hofierka, M. Suri. Open source GIS - GRASS users. Conf., Trento, Italy., 11-13 Sep., (2002).
[28] Http://sel.me.wisc.edu/trnsys.
[29] P. Bourdoukan, E. Wurtz, M. Spérandio, P. Joubert, Build. Simul. (2007) 342–347.